IOP Conf. Series: Materials Science and Engineering **202** (2017) 012001 doi:10.1088/1757-899X/202/1/012001

Spin-Parity Behavior in the Exchange-Coupled Lanthanoid-Nitroxide Molecular Magnets

T Ishida

Department of Engineering Science, The University of Electro-Communications, Chofu, Tokyo 182-8585, Japan

Email: takayuki.ishida@uec.ac.jp

Abstract. To develop lanthanoid-based magnetic materials and relevant devices, reliable prescriptions for molecular/crystal design have long been desired. Ln^{3+}-ion dependence on the molecular magnetism was investigated in the isomorphous series $[Ln(hfac)_3(2pyNO)]$ (Ln = Tb, Dy, Ho, Er), where 2pyNO stands for *tert*-butyl 2-pyridyl nitroxide as a paramagnetic ligand, and hfac for 1,1,1,5,5,5-hexafluoropentane-2,4-dionate. The slow magnetization reversal was evaluated as an indication of single-molecule magnets (SMMs) by out-of-phase ac magnetic susceptibility χ". Whereas the Tb^{3+} ($4f^8$) and Ho^{3+} ($4f^{10}$) derivatives exhibited frequency-dependent χ", practically null χ" was recorded for the Dy^{3+}($4f^9$) and Er^{3+} ($4f^{11}$) derivatives. As for another series with Ln/radical = 1/2, $[Ln(hfac)_3(TEMPO)_2]$ complexes were prepared (Ln = Tb, Dy, Ho, Er, Tm; TEMPO = 2,2,6,6-tetramethylpiperidin-1-oxyl). The Dy^{3+} and Er^{3+} derivatives showed appreciable χ", but the Tb^{3+}, Ho^{3+}, and Tm^{3+} derivatives did not. Thus, the S = 1/2 paramagnetic ligands play a role of a spin-parity switch to regulate whether the compound behaves as an SMM. In the strongly exchange-coupled regime owing to the direct radical coordination bond, the whole molecular electron counting may provide a useful criterion to predict Kramers molecules and accordingly to explore potential SMM candidates.

Keywords: Spin parity, exchange coupling, lanthanoid, nitroxide, molecular, magnet

1. Introduction

Lanthanoid (Ln) elements are many-talented and utilized for commercial magnets and light emitters. To develop lanthanoid-based magnetic materials, media, refrigerants, and relevant devices, reliable prescriptions for molecular/crystal design have long been desired [1-7]. A spin-only $_{64}Gd^{3+}$ ion ($4f^7$) is often chosen as an initial attempt, because of facile comprehension in studies on structure-function relationship [8-14]. The isotropic Gd^{3+} ion leads to simple analysis even with a powder sample. Compared with Gd^{3+}, heavy lanthanoid ions ($_{65}Tb^{3+}$ or heavier) have advantage with an unquenched orbital moment and large magnetic anisotropy. At the second stage of our research strategy, a chemical trend of Ln^{3+} ion series (Ln^{3+}-ion dependence) in the corresponding isomorphous analogs is an important issue for designing various magnets. Single-molecule magnets (SMMs) [1], displaying magnetic hysteresis at the molecular level, have attracted much attention, owing to the paradigm shift in science and engineering of magnets and also to future application in high-density information storage media, quantum computing materials, and other nanodevices.

The mechanism of SMMs is based on the extremely slow magnetization relaxation, which is described by a double-well potential surface with a relatively high activation energy barrier (Δ) (Figure 1). This feature is regulated with the uniaxial magnetic anisotropy and large magnetic moment. Heavy lanthanoid ions ($_{65}Tb^{3+}$, $_{66}Dy^{3+}$, $_{67}Ho^{3+}$, $_{68}Er^{3+}$, and $_{69}Tm^{3+}$ with 8, 9, 10, 11, and 12 electrons in

the 4f orbitals, respectively) are promising candidates for the magnetic source. Furthermore, ions with a half-integer spin are known as a Kramers ion, which guarantees the ground doublet degeneracy. In this sense, it is reasonably accepted that various Dy^{3+}-based SMMs have been well developed [6,15,16]. The class of mononuclear SMMs was later named as single-ion magnets (SIMs) [17]. There have been many SIMs involving Dy^{3+} ions reported to date [18-20]. On the other hand, Tb^{3+} and Ho^{3+}-based magnets require appropriate crystal field effects suitable for the uniaxial magnetic anisotropy and double-well potential energy structure.

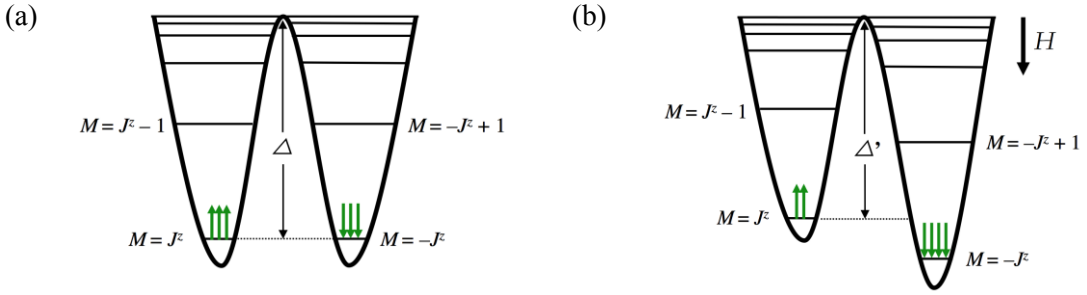

Figure 1. Schematic drawings of a double-well potential surface as a function of J^z (a) without any dc applied field and (b) with a dc bias field.

We have concentrated our attention on 4f-2p heterospin systems and utilized persistent nitroxide radicals (>N-O•) as a paramagnetic ligand. Two kinds of nitroxide radicals will appear in this report; *tert*-butyl 2-pyridyl nitroxdie (2pyNO) [21] and a commercially available spin-probe agent, 2,2,6,6-tetramethylpiperidin-1-oxyl (TEMPO). The 4f spin sources have been selected from heavy-lanthanoid ions. Sterically bulky hfac anions (1,1,1,5,5,5-hexafluoropentane-2,4-dionate) were utilized as a cap and magnetic insulator, so that the resultant complexes are discrete and magnetic properties are ascribable to the single-molecule origin. The even-odd category of electron counting in a whole molecule is switched after an $S = 1/2$ paramagnetic ligand is incorporated. In the present study, we focus on the role of paramagnetic ligands, after overviewing new experimental findings together with some published results.

2. Experimental Method

2.1. Preparation of 2pyNO complexes

Complexes $[Ln(hfac)_3(2pyNO)]$ (abbreviated as **Ln-2pyNO**, hereafter) were prepared as orange platelets or needles from 2pyNO [21] and $[Ln(hfac)_3(H_2O)_2]$ [22] in a dichloromethane-heptane mixed solvent, according to the method known for **Gd-** and **Tb-2pyNO** [8,23,24]. **Dy-2pyNO**: Yield 50%. Mp. 96-98°C. The elemental analysis (C, H, N) of the complex on a PerkinElmer CHNS/O 2400 by a usual combustion method supported the chemical composition. Anal. Calcd.: C, 30.38; H, 1.70; N, 2.95% for $C_{24}H_{16}F_{18}DyN_2O_7$. Found: C, 30.61 H, 1.49; N, 2.97%. IR spectrum (neat; attenuated total reflection (ATR) method on a Nicolet FT-IR spectrometer) 773, 1001, 1059, 1134, 1250, 1648 cm^{-1}. The IR spectra for Ln = Ho, Er are practically the same, irrespective of Ln ions. **Ho-2pyNO**: Yield 53%. Mp. 84-85°C. Anal. Calcd.: C, 30.30; H, 1.70; N, 2.94% for $C_{24}H_{16}F_{18}HoN_2O_7$. Found: C, 30.31 H, 1.44; N, 3.12%. **Er-2pyNO**: Yield 80%. Mp. 85-87°C. Anal. Calcd.: C, 30.23; H, 1.69; N, 2.94% for $C_{24}H_{16}F_{18}ErN_2O_7$. Found: C, 30.13 H, 1.42; N, 3.10%.

2.2. Preparation of TEMPO complexes

Complexes $[Ln(hfac)_3(TEMPO)_2]$ (abbreviated as **Ln-TEMPO$_2$**, hereafter) were prepared as light yellow polycrystals from TEMPO (Tokyo Chemical Industry) and $[Ln(hfac)_3(H_2O)_2]$ [22] in a dichloromethane-heptane mixed solvent, according to the method known for **Gd-** and **Er-TEMPO$_2$** [25,26]. **Tb-TEMPO$_2$**: Yield 55%. Mp. 135–136°C. Anal. Calcd.: C, 36.33; H, 3.60; N, 2.57% for $C_{33}H_{39}F_{18}GdN_2O_8$. Found: C, 36.33; H, 3.55; N, 2.75%. IR spectrum (neat; ATR) 976, 1136, 1253,

1651, 2947 cm^{-1}. The IR spectra for Ln = Dy, Ho, Tm are practically the same, irrespective of Ln ions. **Dy-TEMPO$_2$**: Yield 62%. Mp. 132–133°C. Anal. Calcd.: C, 36.16; H, 3.59; N, 2.56% for $C_{33}H_{39}F_{18}DyN_2O_8$. Found: C, 36.21; H, 3.32; N, 2.67%. **Ho-TEMPO$_2$**: Yield 88%. Mp. 127–128°C. Anal. Calcd.: C, 36.08; H, 3.58; N, 2.55% for $C_{33}H_{39}F_{18}HoN_2O_8$. Found: C, 36.34; H, 3.55; N, 2.69%. **Tm-TEMPO$_2$**: Yield 68%. Mp. 119–120°C. Anal. Calcd.: C, 35.95; H, 3.57; N, 2.54% for $C_{33}H_{39}F_{18}TmN_2O_8$. Found: C, 35.79; H, 3.43; N, 2.69%.

2.3. X-Ray crystallographic analysis

X-ray diffraction data of **Ln-2pyNO** and **Ln-TEMPO$_2$** were collected on a Rigaku Saturn70 CCD diffractometer with graphite monochromated MoKα radiation (λ = 0.71073 Å). The structures were directly solved using a heavy atom method and expanded using Fourier techniques in the *CrystalStructure* program package [27]. All of the hydrogen atoms were refined as "riding." The thermal displacement parameters of the non-hydrogen atoms were refined anisotropically. Selected crystallographic data and geometrical parameters are listed in Tables 1 and 2. CCDC reference numbers are 912946, 1504137, 1504138, and 1504139 for **Tb-**, **Dy-**, **Ho-**, and **Er-2pyNO**, respectively, and 1488109 – 1488113 for **Tb-**, **Dy-**, **Ho-**, **Er-**, and **Tm-TEMPO$_2$**, respectively.

2.4. Magnetic measurements

The alternating-current (ac) magnetic susceptibility of polycrystalline specimens were measured on a Quantum Design PPMS ac/dc magnetometer equipped with a 9 T coil in a temperature range 1.9 – 300 K. Samples were mounted and not fixed in a gelatin capsule. The direct-current (dc) susceptometry was conducted on a Quantum Design MPMS SQUID magnetometer equipped with a 7 T coil in a temperature range 1.8 – 300 K.

3. Results

3.1. 2pyNO complexes

Complexation between [Ln(hfac)$_3$(H$_2$O)$_2$] and 2pyNO in a heptane-dichloromethane mixed solvent afforded [Ln(hfac)$_3$(2pyNO)] (**Ln-2pyNO**) as fine orange polycrystals in moderate yields. The elemental and spectral analyses support the chemical formula. The X-ray diffraction study on **Ln-2pyNO** clarified that the Tb through Er derivatives are completely isomorphous (Figure 2 and Table 1). The space group was triclinic $P\bar{1}$ with Z = 4, and there are two crystallographically independent molecules in a unit cell. The two molecules are similar to each other. The Ln ions are eight-coordinate from one nitrogen and eight oxygen atoms, to form a square antiprism (SAPR), according to the *SHAPE* analysis [28]. The 4f and 2p spin centers are directly bonded in a five-membered chelate ring.

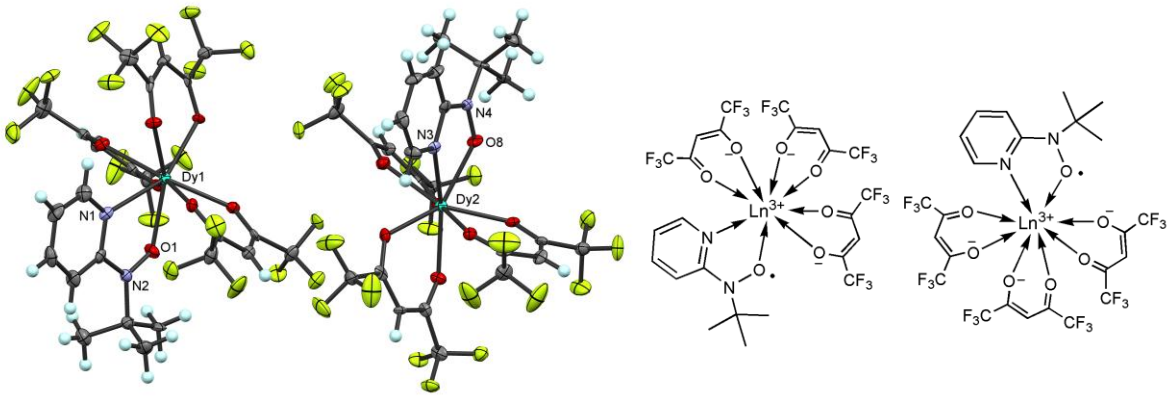

Figure 2. X-Ray crystal structure of two independent molecules of **Dy-2pyNO**. Thermal ellipsoids are drawn at the 50% probability level for non-hydrogen atoms. Structural formula is also shown.

Table 1. Selected crystallographic data of **Ln-2pyNO** (Ln = Tb, Dy, Ho, Er).

	Tb-2pyNO	**Dy-2pyNO**	**Ho-2pyNO**	**Er-2pyNO**
Formula	$C_{24}H_{16}TbF_{18}N_2O_7$	$C_{24}H_{16}DyF_{18}N_2O_7$	$C_{24}H_{16}HoF_{18}N_2O_7$	$C_{24}H_{16}ErF_{18}N_2O_7$
Crystal system	triclinic	triclinic	triclinic	triclinic
Space group	$P\bar{1}$	$P\bar{1}$	$P\bar{1}$	$P\bar{1}$
a / Å	9.491(3)	9.507(2)	9.4973(9)	9.5025(11)
b / Å	15.518(5)	15.515(2)	15.5375(13)	15.540(2)
c / Å	22.240(5)	22.174(3)	22.173(2)	22.144 (3)
α / deg	73.07(2)	72.943(7)	72.817(5)	72.806(5)
β / deg	87.91(2)	87.740(7)	87.723(6)	87.840(6)
γ / deg	88.39(2)	88.364(8)	88.349(6)	88.312(6)
V / Å ^{3}	3131(2)	3123.9(7)	3122.9(5)	3121.0(6)
Z	4	4	4	4
R [a] $(I > 2\sigma(I))$	0.0480	0.0354	0.0662	0.0698
R_w [b] (all)	0.0962	0.0376	0.0736	0.0755
T / K	100	100	100	100
Reference	c)	This work	This work	This work

[a] $R = \Sigma \, ||F_o| - |F_c|| / \Sigma \, |F_o|$. [b] $R_w = [\Sigma \, w(F_o^2 - F_c^2)^2 / \Sigma \, w(F_o^2)^2]^{1/2}$. [c] Murakami R et al. 2013 *Dalton Trans.* **42** 13968.

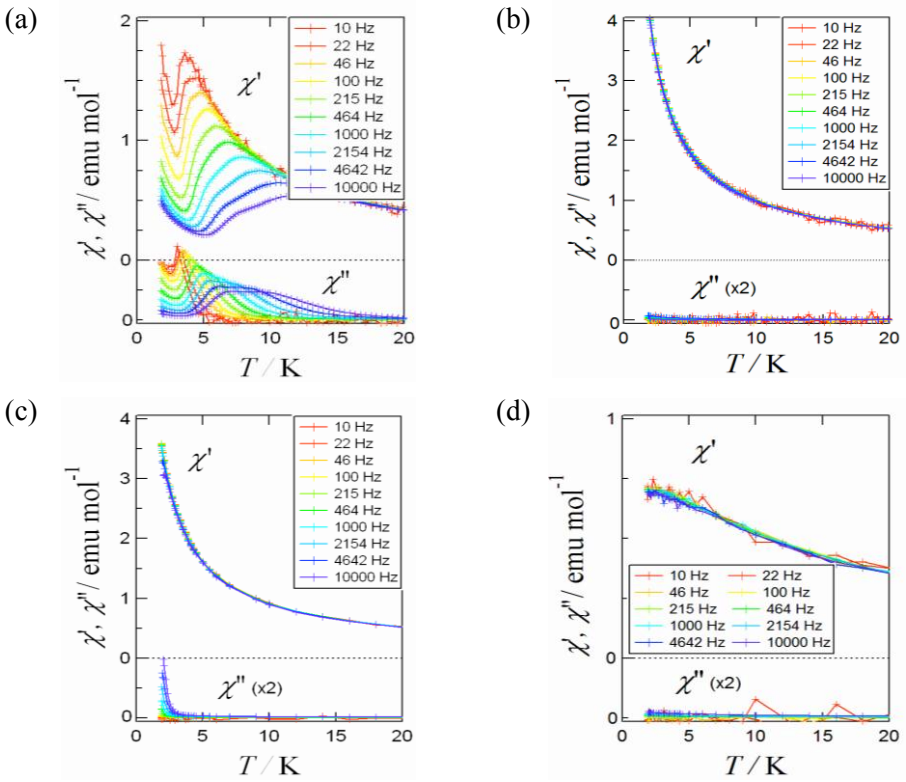

Figure 3. Ac magnetic susceptibilities (top: in-phase χ'; bottom: out-of-phase χ") for (a) **Tb-**, (b) **Dy-**, (c) **Ho-**, and (d) **Er-2pyNO** without any bias field. Lines are shown as a guide to the eyes. Relatively large noises were recorded in the 10 Hz data.

Relatively strong antiferromagnetic coupling was found in **Gd-2pyNO**, originated in the direct Gd-radical coordination bond [8]. The Gd^{3+}-radical exchange coupling constant was determined from the magnetic susceptibility measurements, giving $J_{Gd\text{-}2pyNO}/k_B$ = –13.8(3) K, where the constant is formulated as $H = -J_{Gd\text{-}2pyNO}\, S_{Gd} \bullet S_{2pyNO}$. Study was extended to the heavier lanthanoid ions, but $J_{Ln\text{-}2pyNO}$ could hardly be obtained only from the susceptibility data. Instead, high-field and high-frequency electron paramagnetic resonance spectroscopy and inelastic neutron diffraction study can afford the information of the energy level scheme. Analysis on **Tb-2pyNO** gave $J_{Tb\text{-}2pyNO}/k_B$ = –9.52 and –7.19 K [24]. The sign of exchange coupling is common among the heterospin molecules of Gd^{3+} and heavy Ln^{3+} ions coupled with 3d transition metal ions [29-33] and radicals [24]. The exchange coupling mechanism proposed for Gd compounds [10] seems to hold for the heavier Ln compounds. The intramolecular antiferromagnetic couplings in **Tb-**, **Dy-**, **Ho-**, and **Er-2pyNO** giving a ground ferrimagnetic state were confirmed by the saturation magnetization in the magnetization curves measured at 1.8 K.

The slow magnetization reversal was evaluated with ac magnetic susceptibility. Eventually, **Tb-2pyNO** was characterized as an SMM [23]. Two series of the out-of-phase ac susceptibility (χ") signals appeared around 10 K even at zero direct-current (dc) bias field (Figure 3a), which is consistent with the presence of two independent molecules in a unit cell. The activation energies for the magnetization reversal were estimated as Δ/k_B = 39.2(3) K with $\tau_0 = 4.2(4)\times10^{-8}$ s for one molecule and Δ/k_B = 36(2) K with $\tau_0 = 4.1(12)\times10^{-7}$ s for the other, where τ_0 stands for the pre-exponential factor in the Arrhenius analysis [34]. The Cole-Cole plot [35] supports this argument. On the other hand, unexpectedly, no χ" was recorded for **Dy-2pyNO** (Figure 3b). A Dy^{3+} ion has been supposed to be preferable for development of SMMs because of large magnetic moment and anisotropy, and moreover the Kramers theorem tells us that the half-integer spin ($S_{Dy^{3+}}$ = 5/2) would bring about the double-well potential. As for the Ho^{3+} analog, **Ho-2pyNO** exhibited appreciable χ" with frequency dependence (Figure 3c), though a Ho^{3+} ($S_{Ho^{3+}}$ = 2) ion is not a Kramers ion. The Er^{3+} ($S_{Er^{3+}}$ = 3/2) derivative, **Er-2pyNO**, did not show any meaningful χ" (Figure 3d). The present chemical trend indicates that an even-odd effect regulates the SMM characteristics and that a paramagnetic ligand with S = 1/2 switches the even-odd classification on electron counting.

3.2. TEMPO complexes

As a series with a Ln/radical ratio of 1/2, $[Ln(hfac)_3(TEMPO)_2]$ complexes have been prepared and characterized. Complexation between $[Ln(hfac)_3(H_2O)_2]$ and TEMPO afforded **Ln-TEMPO$_2$** as light yellow crystalline products in moderate yields. The elemental and spectral analyses support the chemical composition. The X-ray diffraction study on **Ln-TEMPO$_2$** clarified that all the derivatives are isomorphous (Figure 4 and Table 2). The Ln ions are coordinated by eight oxygen atoms, consisting of two from TEMPO nitroxides and six from three diketonate groups. The *SHAPE* [28] analysis clarified that the coordination polyhedron belongs to a triangular dodecahedron (TDD). Two TEMPO groups are located at "*trans*" positions with respect to the Ln center, and the two TEMPO ends are well separated with three hfac groups. In a crystal, the peripheral CF_3 and TEMPO alkyl groups magnetically isolate adjacent molecules.

Relatively strong exchange coupling was observed for **Gd-TEMPO$_2$** with $J_{Gd\text{-}TEMPO}/k_B$ = –12.9(5) and +8.0(6) K although TEMPO---TEMPO exchange coupling would disturb the analysis [25]. A chemical trend was investigated also in this series, and dominant antiferromagnetic $J_{Ln\text{-}TEMPO}$ couplings were proven from the saturation magnetization in the magnetization curve measurements [26]. As for the Kramers-ion analogs, **Dy-** and **Er-TEMPO$_2$** showed an indication of an SMM, as frequency-dependent χ" was recorded (Figure 5). The crystal field parameters were evaluated for **Er-TEMPO$_2$**, and considerably large Er^{3+}-radical exchange couplings have been pointed out [26]. The χ" upsurge observed for **Er-TEMPO$_2$** is only slight, but substantial as shown in the dc bias field experiments [26]. In contrast, practically null χ" was recorded for **Tb-**, **Ho-**, and **Tm-TEMPO$_2$**.

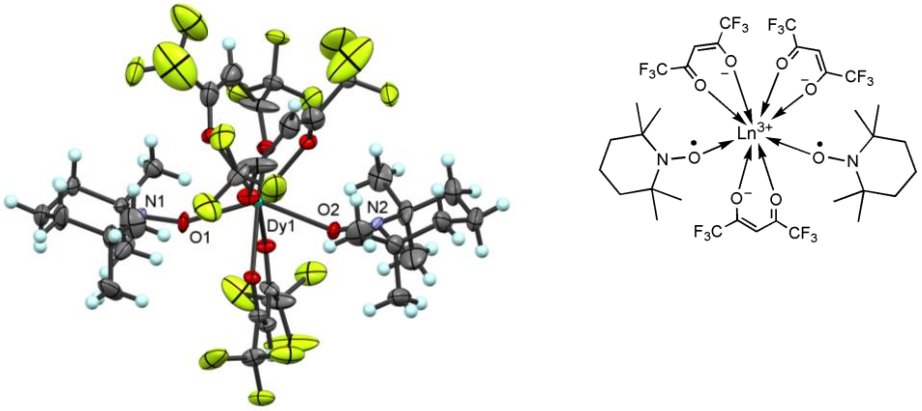

Figure 4. Molecular structure of (a) **Dy-TEMPO$_2$**. Thermal ellipsoids are drawn at the 50% probability level for non-hydrogen atoms. Structural formula is also shown.

Table 2. Selected crystallographic data of **Ln-TEMPO$_2$** (Ln = Tb, Dy, Ho, Er, Tm).

	Tb-TEMPO$_2$	**Dy-TEMPO$_2$**	**Ho-TEMPO$_2$**	**Er-TEMPO$_2$**	**Tm-TEMPO$_2$**
Formula	$C_{33}H_{39}Tb$-$F_{18}N_2O_8$	$C_{33}H_{39}Dy$-$F_{18}N_2O_8$	$C_{33}H_{39}Ho$-$F_{18}N_2O_8$	$C_{33}H_{39}Er$-$F_{18}N_2O_8$	$C_{33}H_{39}Tm$-$F_{18}N_2O_8$
Crystal system	momoclinic	momoclinic	momoclinic	momoclinic	momoclinic
Space group	$P2_1/c$	$P2_1/c$	$P2_1/c$	$P2_1/c$	$P2_1/c$
a / Å	11.980(3)	11.970(3)	11.9648(13)	11.943(3)	11.937(2)
b / Å	16.158(4)	16.150(4)	16.152(2)	16.145(4)	16.133(3)
c / Å	22.288(6)	22.249(5)	22.255(3)	22.015(4)	22.195(4)
β / deg	90.98(1)	91.04(1)	90.9350(9)	90.981(9)	91.0296(10)
V / Å^3	4314(2)	4300(2)	4300.4(8)	4283(2)	4273.6(12)
Z	4	4	4	4	4
R [a] ($I > 2\sigma(I)$)	0.0607	0.0602	0.0686	0.0626	0.0640
R_w [b] (all)	0.0854	0.1013	0.1248	0.0793	0.1099
T / K	100	100	100	100	100
Reference	This work	This work	This work	c)	This work

[a] $R = \Sigma \, ||F_o| - |F_c|| / \Sigma \, |F_o|$. [b] $R_w = [\Sigma \, w(F_o^2 - F_c^2)^2 / \Sigma \, w(F_o^2)^2]^{1/2}$. [c] Karbowiak M et al. 2016 *Chem. Phys. Lett.* **662** 163.

To compare the specification values of **Dy-** and **Er-TEMPO$_2$**, we performed the ac magnetic susceptibility measurements on **Dy-TEMPO$_2$** under the same conditions; namely, a dc bias field of 1000 Oe was applied to prevent possible quantum tunneling of the magnetization (Figure 1b). An obvious frequency dependence was recorded (Figure 6a). As the Arrhenius plot shows (Figure 6b), a downward deviation of the data points from the Arrhenius expectation is found below 2.5 K, suggesting the presence of a Raman-type relaxation and/or residual quantum tunneling process. In the Arrhenius regime, the activation energy for the magnetization reorientation for **Dy-TEMPO$_2$** was estimated as $\Delta/k_B = 24(1)$ K with $\tau_0 = 1.2(5) \times 10^{-8}$ s, while $\Delta/k_B = 18.2(19)$ K with $\tau_0 = 9(5) \times 10^{-8}$ s for **Er-TEMPO$_2$** [26]. The activation energy of **Dy-TEMPO$_2$** is larger than that of **Er-TEMPO$_2$**. The Cole-Cole plot on the $T = 2.0$ and 3.0 K data afforded $\alpha = 0.29(1)$ and 0.26(2), respectively (for the definition of α, see [36]). The presence of single relaxation process is indicated, and it becomes clearer when $T = 3.0$ K than when $T = 2.0$ K (Figure 6c). We have to stress that **Dy-** and **Er-TEMPO$_2$** behaved as a typical SMM. The present chemical trend reveals an even-odd effect, and the even-odd classification of **Ln-TEMPO$_2$** is just the same as that of Ln^{3+} single ions.

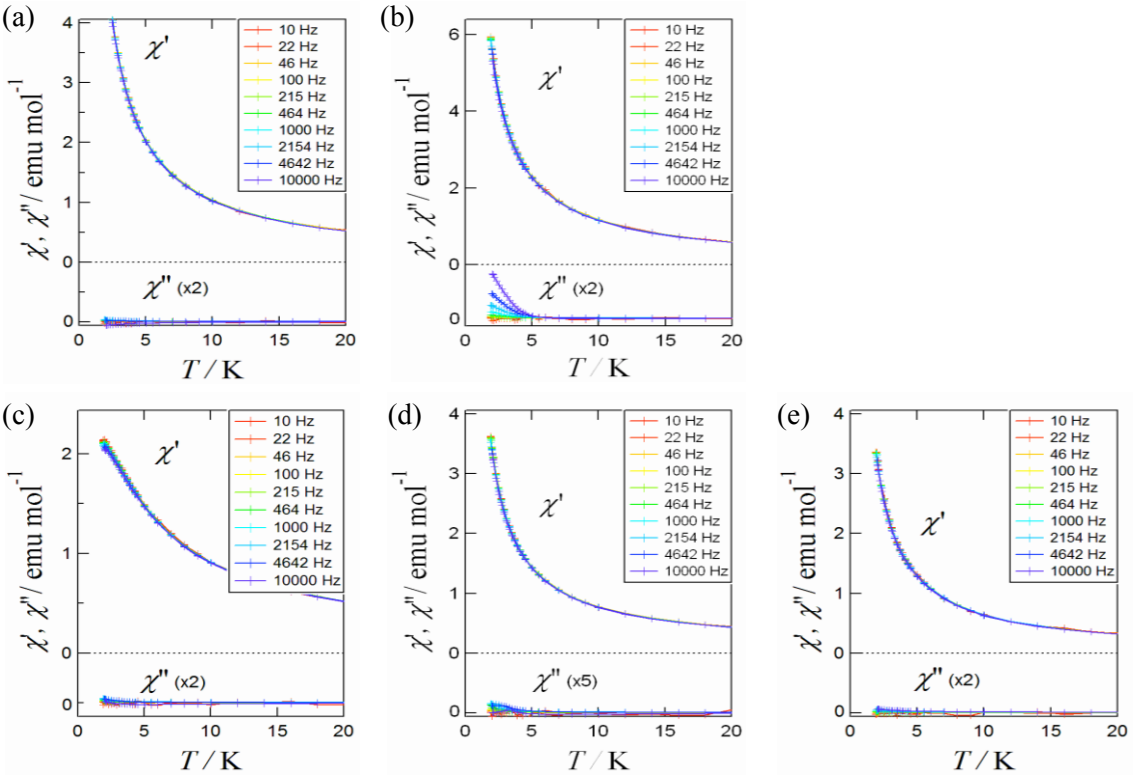

Figure 5. Ac magnetic susceptibilities (top: in-phase χ'; bottom: out-of-phase χ") for (a) **Tb-**, (b) **Dy-**, (c) **Ho-**, (d) **Er-**, and (e) **Tm-TEMPO$_2$** without any bias field. Lines are shown as a guide to the eyes.

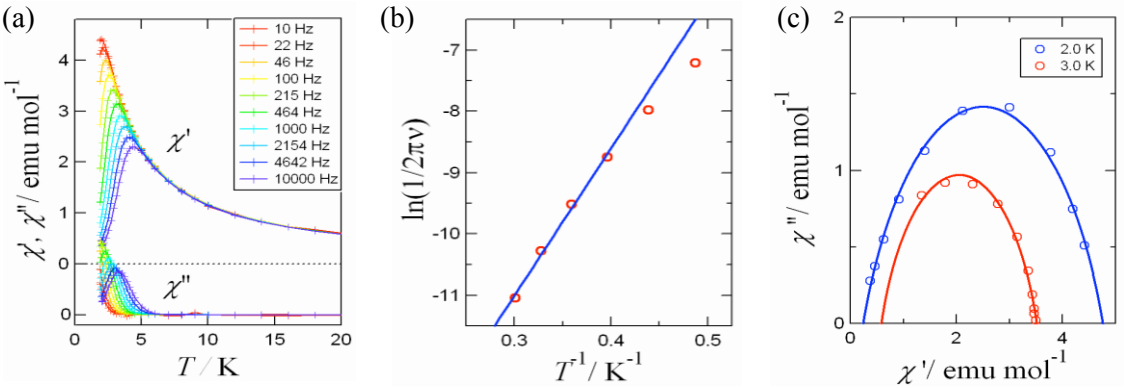

Figure 6. (a) Ac magnetic susceptibilities measured for **Dy-TEMPO$_2$** with a dc bias field of 1000 Oe. (b) The Arrhenius plot and (b) the Cole-Cole plot of the data taken from (a).

4. Discussion

All the compounds investigated here possess a ferrimagnetic ground state, and each molecule with the residual magnetic moment behaves as a paramagnet. During the screening of SMMs by means of ac susceptometry, a clear empirical rule emerges. The paramagnetic ligands play a role of a spin-parity switch to regulate whether the complex behaves as a potential SMM or not.

In the Ln/radical = 1/1 families, SMM behavior was observed for **Tb-2pyNO** [23] and **Tb-6bpyNO** [37] but not for **Dy-2pyNO** or **Dy-6bpyNO** (6bpyNO is a derivative of 2pyNO, 2,2'-bipyridin-6-yl *tert*-butyl nitroxide [38]; for the structural formula, see Figure 6). The electron countings of the whole molecule are odd for the Tb-radical compounds and even for the Dy-radical

compounds. Similarly, the whole electron countings are odd for **Ho-2pyNO** and even for **Er-2pyNO**. Replacing the paramagnetic ligand with a diamagnetic one gave additional evidence [37]. Namely, **Tb-6bpyCO** is not an SMM despite having practically the same crystal field (6bpyCO = 2,2'-bipyridin-6-yl *tert*-butyl ketone; Figure 7). Since **Dy-2pyNO**, **Dy-6bpyNO**, and **Tb-6bpyCO** were not an SMM, the crystal field is unimportant to design SMMs in these systems.

The results on **Ln-TEMPO$_2$** with Ln/radical = 1/2 are completely different from those of **Ln-2pyNO**; **Dy-** and **Er-TEMPO$_2$** showed an indication of an SMM, whereas almost zero χ" was recorded for **Tb-**, **Ho-**, and **Tm-TEMPO$_2$**. Supporting evidence was given from the study on **Ln-TMIO$_2$** [39] (TMIO = 1,1,3,3-tetramethylisoindolin-2-oxyl; Figure 7). Two paramagnetic ligands in a molecule are symmetrically related, and Tb- and Dy-radical antiferromagnetic couplings have been evaluated by means of electron paramagnetic resonance spectroscopy [40]. A Kramers molecule **Dy-TMIO$_2$** displayed distinct frequency-dependent χ" with a 1000 Oe dc bias field, and a non-Kramers molecule **Tb-TMIO$_2$** did not [40]. The presence of two S = 1/2 paramagnetic ligands maintains the even-odd classification of the whole molecular electron counting. Consequently the experimental results are totally compatible with the Kramers theorem. The bistability is not guaranteed for a non-Kramers Tb^{3+} ion, and actually **Tb-TEMPO$_2$** and **Tb-TMIO$_2$** exhibited flat χ". The present finding indicates that the crystal field effect is not a decisive factor to bestow an SMM character to these systems.

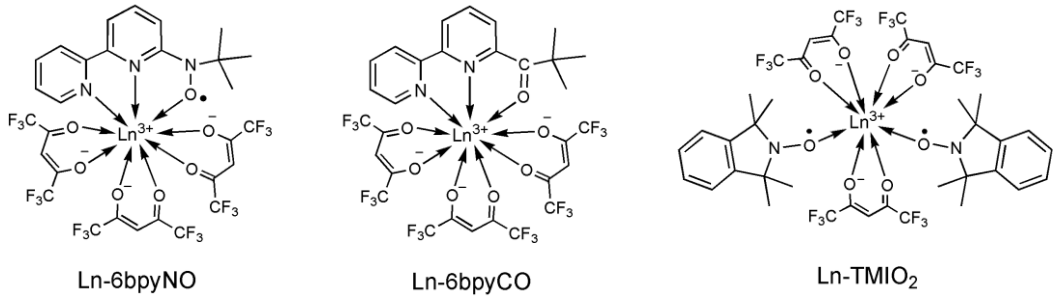

Figure 7. Structural formulas of **Ln-6bpyNO**, **Ln-6bpyCO**, and **Ln-TMIO$_2$**.

In the strongly exchange-coupled systems having the direct radical coordination, the total spin may be a useful criterion to predict Kramers molecules. It is noticed at the present stage that the integer or half-integer of the total spin is essential, regardless of the angular momentum. The *LS* coupling is defined within a single ion whereas the spin-spin coupling works between two paramagnetic centers or more. When the latter is stronger than the former, the coupling scheme of the spin-spin coupling first and the *LS* coupling later might be a possible explanation. In the heavy Ln group, L and S point to the same direction, i.e., $J = L + S$. After the spin-spin antiferromagnetic coupling is operative, the Ln total moment and radical moment are antiferromagnetically correlated. The Kramers theorem is a useful criterion to find SMM candidates, assuming that the spin-spin coupling is strong enough (typically in the order of 10 K), compared with cryogenic temperatures (e.g. 4.2 K). Such a discrimination method is not valid for 4f-3d or 4f-4f systems, because their spin-spin couplings are comparably small (typically in the order of 1 K or smaller).

Although a simple spin-parity behavior has already been reported for the DOTA-based SIMs [41] (DOTA = 1,4,7,10-tetraazacyclododecane-1,4,7,10-tetraacetic acid), an example of 4f-2p heterospin compounds is unprecedented. The establishment of the spin-parity effect on SMMs [42] needs detailed experiments on dynamics and theoretical consideration. If a factor of the tunneling probability at zero applied field is removed or focused on, experiments with dc bias fields would afford a clue, and each possible relaxation process should be separated and evaluated. So far, such measurements revealed a qualitatively unchanged trend for **Ln-2pyNO**, **Ln-TEMPO$_2$**, and **Ln-TMIO$_2$** at a bias field of 1000 Oe and for **Ln-6bpyNO** and **Ln-6bpyCO** at a bias field of 2000 Oe. Absorption and emission

measurements will clarify the energy level structure with the crystal field splitting. Further studies are now underway.

5. Conclusion

The present study unveils the role of the paramagnetic ligand incorporated in 4f-2p heterospin systems. When 4f-2p heterospin compounds possess sizable exchange coupling due to the direct radical coordination, a quite unique situation is realized. In the strongly exchange coupling regime, the whole molecular electron counting provides a useful criterion to predict Kramers doublet molecules and accordingly to search for potential SMM candidates. The control of the relaxation time constants by means of introduction of a paramagnetic ligand would lead to new tactics in designing 4f-based molecules toward novel SMMs, data storage media, and quantum computing devices.

6. References

[1] Gatteschi D, Sessoli R and Villain J 2006 *Molecular Nanomagnets*, Oxford University Press, New York
[2] Demir S, Jeoh I–R, Long J R, Harris T D 2015 *Coord. Chem. Rev.* **289** 149
[3] Andruh M, Costes J P, Diaz C and Gao S 2009 *Inorg. Chem.* **48** 3342
[4] Liu K, Shi Wand Cheng P 2015 *Coord. Chem. Rev.* **289-290** 74
[5] Bogani L, Sangregorio C, Sessoli R and Gatteschi D 2005 *Angew. Chem. Int. Ed.* **44** 5817
[6] Reinhart J D and Long J R 2011 *Chem. Sci.* **2** 2078
[7] Suarez A I O, Lyaskovskyy V, Reek, J N H, van der Vlugt J I and de Bruin B 2013 *Angew. Chem. Int. Ed.* **52** 12510
[8] Ishida T, Murakami R, Kanetomo and T, Nojiri H 2013 *Polyhedron* **66** 183
[9] Kanetomo T and Ishida T 2014 *Inorg. Chem.* **53** 10794
[10] Kanetomo T, Yoshitake T and Ishida T 2016 *Inorg. Chem.* **55** 8140
[11] Kanetomo T and Ishida T 2014 *Chem. Commun.* **50** 2529
[12] Kanetomo T and Ishida T 2016 *AIP Conf. Proc.* **1709** 020015
[13] Nakamura T and Ishida T 2016 *AIP Conf. Proc.* **1709** 020016
[14] Ikegaya N, Kanetomo T, Murakami and R, Ishida T. 2012 *Chem. Lett.* **41** 82
[15] Zhang P, Guo Y-N and Tang J 2015 *Coord. Chem. Rev.* **257** 1728
[16] Mori F, Nyui T, Ishida T, Nogami T, Choi K-Y and Nojiri H 2006 *J. Am. Chem. Soc.* **128** 1441
[17] Ishikawa N, Sugita M, Ishikawa T, Koshihara S Y and Kaizu Y 2003 *J. Am. Chem. Soc.* **125** 8694
[18] Cucinotta G, Perfetti M, Luzon J, Etienne M, Car P-E, Caneschi A, Calvez G, Bernot K and Sessoli R 2012 *Angew. Chem. Int. Ed.* **51** 1606
[19] Jiang S-D, Wang B-W, Su G, Wang Z-M and Gao S 2010 *Angew. Chem. Int. Ed.* **41** 7448
[20] Watanabe A, Yamashita A, Nakano M, Yamamura T and Kajiwara T 2011 *Chem. Eur. J.* **17** 7428
[21] Okazawa A, Nogami T and Ishida T 2007 *Chem. Mater.* **19** 2733
[22] Richardson M F, Wagner W F and Sands D E 1968 *J. Inorg. Nucl. Chem.* **30** 1275
[23] Murakami R, Ishida T, Yoshii S and Nojiri H 2013 *Dalton Trans.* **42** 13968
[24] Baker M L, Tanaka T, Murakami R, Ohira-Kawamura S, Nakajima T, Ishida T and Nojiri H 2015 *Inorg. Chem.* **54** 5732
[25] Murakami R, Nakamura T and Ishida T 2014 *Dalton Trans.* **42** 5893
[26] Karbowiak M, Rudowicz C, Nakamura T, Murakami R and Ishida T 2016 *Chem. Phys. Lett.* **662** 163
[27] *CrystalStructure* ver. 4.0. 2010 Rigaku Corp. Tokyo, Japan
[28] *SHAPE* v2.1. Lluncll M, Casanova D, Circra J, Bofill J M, Alcmany P, Alvarez S, Pinsky, M, Avnir D, University of Barcelona and The Hebrew University of Jerusalem, Barcelona, 2005
[29] Kobayashi Y, Ueki S, Ishida T and Nogami T 2003 *Chem. Phys. Lett.* **378** 337
[30] Ueki S, Ishida T, Nogami T, Choi K-Y and Nojiri H 2007 *Chem. Phys. Lett.* **440** 263
[31] Ueki S, Kobayashi Y, Ishida T and Nogami T 2005 *Chem. Commun.* 5223

[32] Okazawa A, Nogami T, Nojiri H and Ishida T 2008 *Chem. Mater.* **20** 3110
[33] Okazawa A, Watanabe R, Nojiri H, Nogami T and Ishida T 2009 *Polyhedron* **28** 1808
[34] Sessoli R, Tsai H-L, Schake A R, Wang S, Vincent J B, Folting K, Gatteschi D, Christou G and Hendrickson D N 1993 *J. Am. Chem. Soc.* **115** 1804
[35] Cole K S, Cole H R 1941 *J. Chem. Phys.* **9** 341
[36] Sessoli R and Powell A K 2009 *Coord. Chem. Rev.* **253** 2328
[37] Kanetomo T, Yoshii S, Nojiri H and Ishida T 2015 *Inorg. Chem. Front.* **2** 860
[38] Osanai K, Okazawa A, Nogami T and Ishida T 2006 *J. Am. Chem. Soc.* **128** 14008
[39] Nakamura T and Ishida T 2015 *Polyhedron* **87** 302
[40] Ishida T, Nakamura T, Kihara T and Nojiri H 2017 *Polyhedron in press* (doi:10.1016/j.poly.2017.03.008).
[41] Boulon M-E, Cucinotta G, Luzon J, Degl'Innocenti C, Perfetti N, Bernot K, Calvez G, Caneschi A and Sessoli R 2013 *Angew. Chem. Int. Ed.* **52** 350
[42] Wernsdorfer W, Chakov N E and Christou G 2005 *Phys. Rev. Lett.* **95** 037203

Acknowledgments
This work has been carried out in collaboration with Dr. Kanetomo T, Mr. Nakamura T, and Ms. Murakami R. The author thanks Prof. Nojiri H (IMR, Tohoku Univ.) for valuable discussion. This work was financially supported by KAKENHI (Grant Number JSPS/15H03793).